Experimental Study of the Multi-Row Disk Inlet

Yusuke Maru
Graduate Student of Engineering, The University of Tokyo
3-1-1 Yoshinodai, Sagamihara Kanagawa 229-8510 Japan
E-mail: yusuke@pub.isas.jaxa.jp

Hiroaki Kobayashi, Takayuki Kojima, Tetsuya Sato and Nobuhiro Tanatsugu
Institute of Space Technology and Aeronautics (ISTA), Japan Aerospace Exploration Agency (JAXA)

Keywords: supersonic, axi-symmetric inlet, conical cavity flow, Multi-Row Disk inlet

Abstract

In this paper are presented a concept of a new supersonic air inlet, which is designated a Multi-Row Disk (MRD) inlet, aiming at performance improvement under off-design conditions, and results of wind tunnel tests examined performance characteristics of the MRD inlet. The MRD inlet is frequently called 'a skeleton inlet' because of its appearance. The performance of a conventional axi-symmetric inlet with a solid center body (spike) deteriorates under off-design Mach number conditions. It is due to the fact that total pressure recovery (TPR) governed by the throat area of inlet and mass capture ratio (MCR) governed by an incidence position of an oblique shock from the spike tip into the cowl can not be controlled independently in such air inlet. The MRD inlet has the spike that is composed of a tip cone and several disks arranged downstream of it, based on the experimental fact that several deep cavities on a conical surface have little negative effect on the boundary layer growth. The overall spike length of the MRD inlet is adjustable to the given flight speed by changing space between disks so that a spillage flow can be controlled independently from controlling the throat area. It could be made clear from the result of wind tunnel tests that the MRD inlet improves TPR by 10% compared with a conventional inlet with a solid spike under off-design conditions.

Introduction

The Institute of Space and Astronautical Science (ISAS), unified into Japan Aerospace Exploration Agency (JAXA) with NAL and NASDA, has developed ATREX engine (Fig.1) as a propulsion system of a fly-back booster on a reusable TSTO space plane[1]. The ATREX engine is a precooled Expander cycle Air-Turbo Ramjet engine using liquid hydrogen as fuel and coolant. This engine has a large supersonic inlet which is installed upstream of a core-engine in order to capture and compress an incoming air. Performances related to engine weight, such as specific impulse and thrust to weight ratio, are very important in an air-breathing for the future space plane, unlike that for airplanes. Therefore, the ATREX engine adopts an axi-symmetric inlet that can reduce structure weight compared with a rectangular (two-dimensional) inlet.

The air-breathing engines for the space plane are operated under a wide range of Mach number from lift-off to about Mach 6 with an accelerating flight conditions. Therefore, its air inlet geometry must be variable in order to form the optimum flow channel according to the variable flight velocity. The installation of a variable mechanism on the axi-symmetric inlet is one of the weak points of axi-symmetric inlets. Up to now, few variable mechanisms have been proposed, e.g. the mechanism translating the inlet centerbody forward and backward, adopted in the inlet of SR-71 Blackbird[2], and changing the diameter of the centerbody, adopted in the VDC inlet by NASA GRC[3-4]. The inlet of the ATREX engine adopts the mechanism that translates a centerbody. Since 1993, a development study of the axi-symmetric variable geometry air inlet has been conducted experimentally and numerically in ISAS[5-7].

From the studies about ATREX inlets, the characteristic of the conventional axi-symmetric variable geometry air inlet for the future space plane is considered and its some weak points are designated. We propose a new air inlet that can overcome those weak points of the conventional inlet and conducts the wind tunnel tests to verify it.

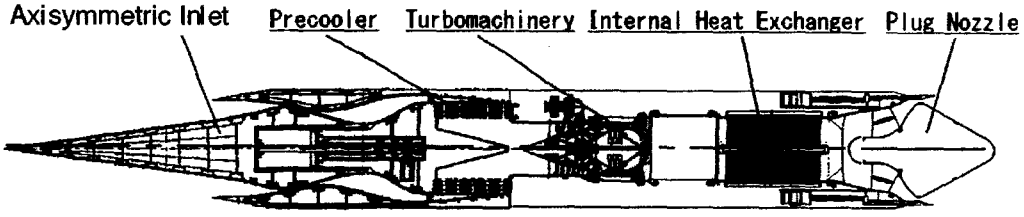

Fig. 1 Schematic view of the ATREX engine with the conventional axi-symmetric inlet.

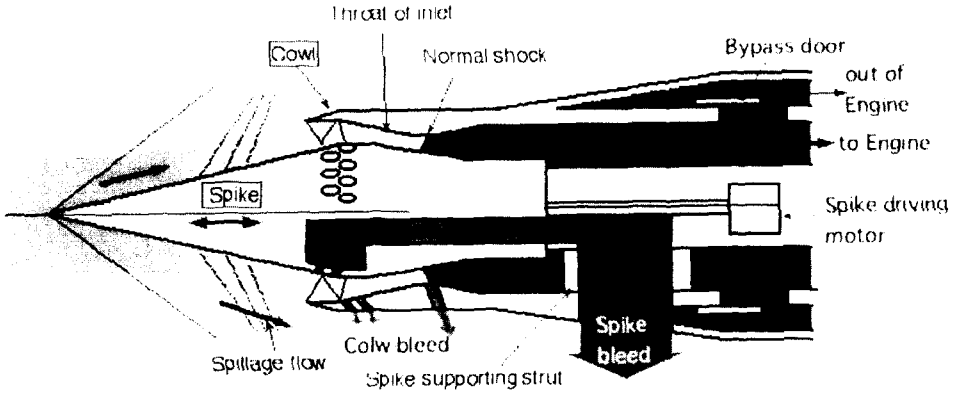

Fig.2 Schematic drawing of the axi-symmetric variable geometry air inlet.

Characteristic of the Conventional Axi-symmetric Variable Geometry Air Inlet

Figure 2 shows a schematic drawing of the axi-symmetric variable geometry air inlet. It mainly consists of two components: a centerbody called 'a spike' and a cowl. Generally, performance of the air inlet is evaluated by two parameters defined as follows; Total Pressure Recovery (TPR) is defined as a ratio of a total pressure of the air captured by the inlet to a total pressure of the free stream. Mass Capture Ratio (MCR) is defined as a ratio of a mass flow swallowed through the inlet throat to a mass flow through the cowl inlet area in the free stream.

The total pressure loss mainly occurs through the normal shock that changes supersonic flow into subsonic. The throat area should be variable according to the free stream Mach number in order to get high TPR with keeping the suitable contraction ratio. That is to say, TPR is governed by the throat area. On the other hand, the loss of mass flow depends mainly on the spillage flow from a gap between the oblique shock wave generated from the spike tip and the cowl lip, shown as Fig.2. That is to say, MCR is governed by the incident position of the oblique shock from the spike tip into the cowl. As the throat area of the conventional axi-symmetric inlet is adjusted in order to get high TPR by translating the overall spike, the oblique shock position that governs MCR is determined simultaneously. Thus TPR and MCR cannot be controlled independently on the conventional axi-symmetric inlet with the solid centerbody. Consequently, the off-design performance would be deteriorated as follows. The inlet geometry is generally designed as the oblique shock wave from the spike tip attaches the cowl lip ('shock-on-lip condition') at the maximum operated Much number M_{design}. When the flight Mach number M_∞ is below M_{design}, the oblique shock is detached from the cowl lip, which causes a decrease of MCR, by translating centerbody forward to set the adequate contraction ratio as shown in Fig. 3. Because MCR is determined according to the adjusted throat area that keeps high TPR, a mass flow rate breathed by the inlet is more than that required by the core-engine. Hence, the surplus mass flow must be discharged out of engine through a bypass door. Such bypass flow is inefficient for the engine system because it only causes ram-drag to the engine without giving thrust.

In order to improve the off-design performance of the axi-symmetric air inlet, we invented a new axi-symmetric air inlet with a new spike configuration and a variable geometry mechanism.

Concept of the Multi-Row Disk Inlet

A new axi-symmetric air inlet is designated as Multi-Row Disk (MRD) inlet[8-10]. The centerbody of the MRD inlet is composed of a tip cone and

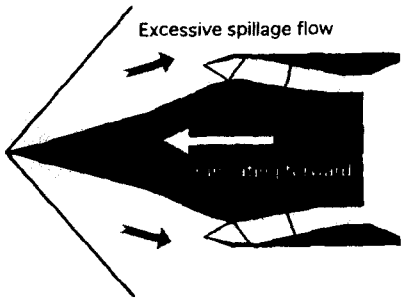

(a) Low Speed Operation ($M_\infty < M_{design}$)

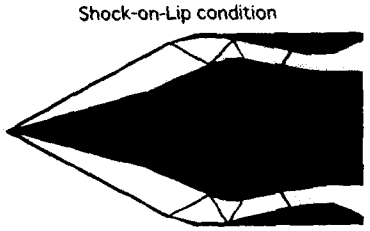

(b) High Speed Operation ($M_\infty = M_{design}$)

Fig. 3 Schematic drawing of flow field around conventional axi-symmetric air inlet.

several disks arranged downstream as shown in Fig. 4. The MRD inlet is called 'skeleton inlet' because of its appearance. Because the overall spike length can be adjusted by changing disk spacing, TPR governed by the throat area and MCR governed by the incidence position of the oblique shock from spike tip into the cowl can be controlled independently. This function has been never seen on the conventional axi-symmetric air inlets.

Improvement of the inlet performance under the off-design condition can be achieved by controlling TPR, or compression ratio, and MCR independently. In case of decreasing MCR and increasing compression ratio, the rear part of the spike is translated backward while front part forward by making disk spacing wide, i.e. the overall spike length is expanded in axial direction as shown in Fig.4 (a). On the contrary, in order to increase MCR and decrease the compression ratio, the front part of the spike is translated backward while rear part forward by making disk spacing narrow, i.e. the overall spike length is truncated as shown in Fig.4 (b). Ideally, MCR would be always 100% if the spike length were controlled so that shock-on-lip condition is achieved. However, the conical cavity flow formed in-between disks may have a negative influence upon the boundary layer profiles resulting in the deteriorated on-design performance of the inlet.

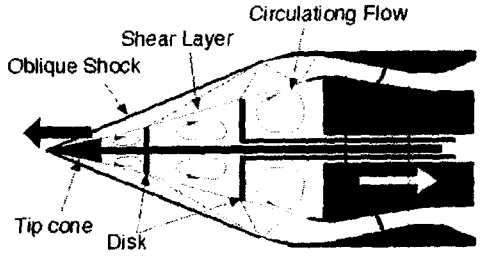

(a) MRD inlet with expanded spike

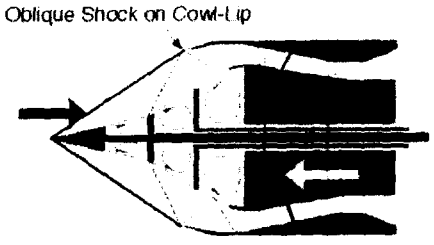

(b) MRD inlet with truncated spike

Fig.4 Conceptual view of the MRD inlet.

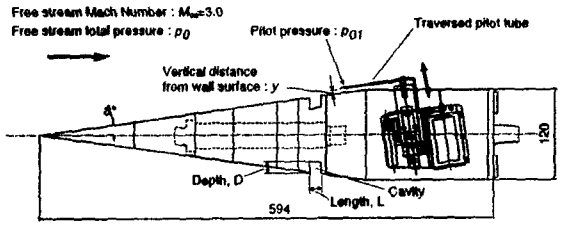

Fig.5 Schematic drawing of test model of the cone for investigating conical cavity flow characteristics.

Investigation of the Conical Cavity Flow Characteristics

The MRD inlet has several cavities on its spike surface. There have been many researches concerning to the cavity flow on a plate[11-14]. However, there are few researches concerning to the conical cavity flow. Therefore, supersonic wind tunnel tests for investigating the characteristics of conical cavity flow are conducted as the first step of this study.

Experimental Apparatus and conditions

Figure 5 shows the schematic drawing of the wind tunnel test model. This model, whose base cylinder diameter is 120 mm, has a right circular cone with its half-cone-angle of 8 degrees. Several types of the cavity can be set on the cone surface. Boundary layer profiles are measured with a traversed pitot tube. Schlieren visualization systems are equipped to watch the front end of the model. Cavity L/D, which is defined as the ratio of the cavity length L to its depth D as shown in Fig.5, cavity size and the number of cavities were considered as experimental parameters. This test was conducted in ISAS supersonic wind tunnel, on which the free stream Mach number is 3.0. Experimental conditions are summarized in Table.1

Experimental Results

Figure 6 shows Schlieren images of the conical cavity flow. From these images, shear layers passing over cavities are observed. Such flow is called 'open cavity flow'. In case of the shallow cavity (i.e. cavity L/D is large), an oblique shock wave from the leading edge of the cavity due to shear layer turning and another from the tailing edge due to the flow hitting the cavity rear face are strong. On the other hand, oblique shock waves on the cavity with the small cavity L/D are weak. This is because the internal pressure of the deep cavity decreases and the turning of shear layer becomes small.

Figure 7 (a) shows the pitot pressure distribution with changing the cavity L/D, while a cavity depth D and the number of cavities N were fixed such as D = 15 mm and N=1. Total pressure loss increases and the boundary layer becomes thicker due to the shock waves generated from the leading edge and tailing edge of the cavity. However, if L/D is enough small (less than 1), the change of total pressure loss is negligible. Figure 7 (b) shows the results in case of varying the cavity size and number, where L/D = 1. The trend of total pressure loss is less affected by the cavity size and the number of cavities compared with the cavity L/D. From these findings, it is expected that addition of several cavities with the small L/D on the spike hardly affect the inlet flow field.

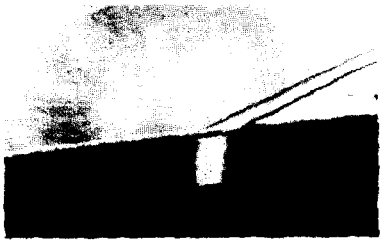

(a) Single cavity, L/D=1, D=15 mm.

(b) Single cavity, L/D=0.5, D=15

(c) Single cavity, L/D=3.7, D=15

(d) Two cavities, L/D=1, D=15

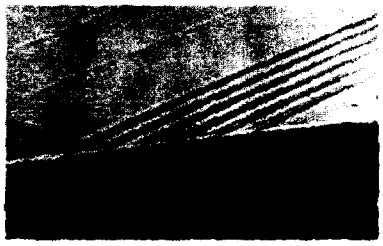

(e) Six cavities, L/D=1, D=5

Fig. 6 Schlieren image of flow field around conical cavity.

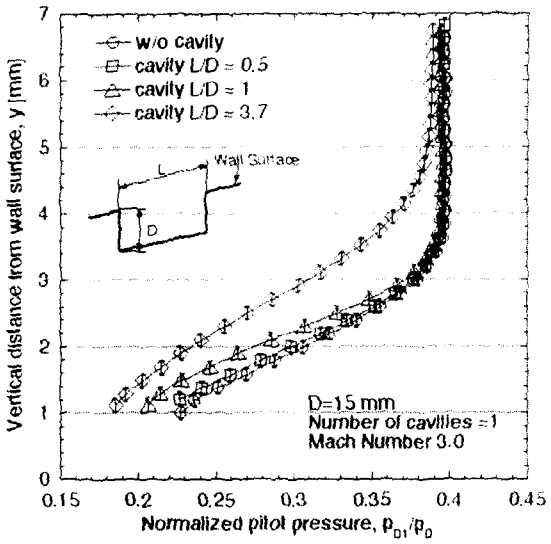

(a) Parameter: the cavity L/D.

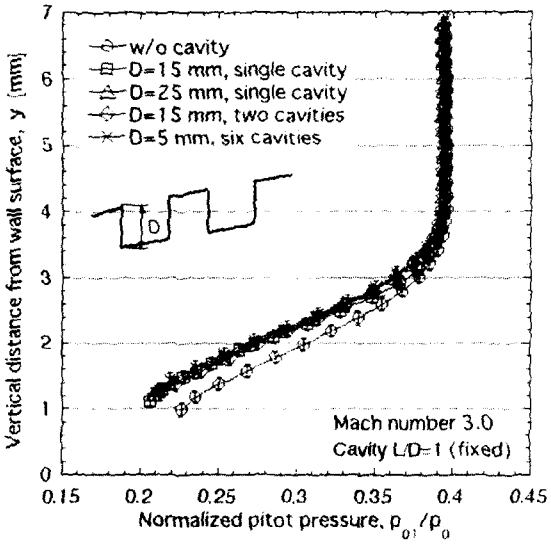

(b) Parameter: the size and the number of cavities.

Fig. 7 Pitot pressure distribution downstream of cavities.

Validation Tests of the MRD Inlet

Wind tunnel tests were conducted in order to validate several merits of the MRD inlet and extract problems peculiar to the MRD inlet in ISAS supersonic wind tunnel under Mach 3.5 and 4.0 conditions and in Institute of Space Technology and Aeronautics (ISTA) hypersonic wind tunnel under Mach 5.1 condition.

Experimental Apparatus and Conditions

Figure 9 shows a schematic drawing of the validation test model. The model drawn in Fig.9 (a) was tested in ISAS wind tunnel and that drawn in Fig.9 (b) in ISTA wind tunnel. Figure 10 shows a photograph of the model installed in ISTA wind

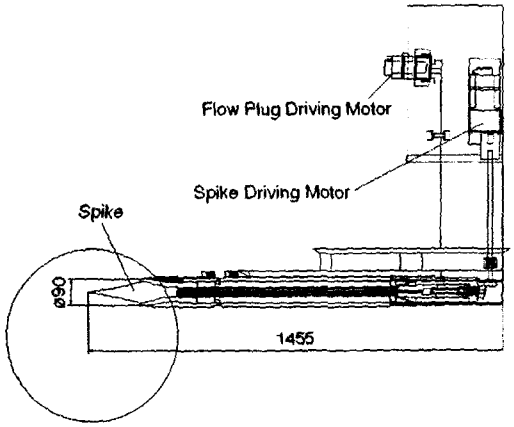

(a) Model tested in ISAS supersonic wind

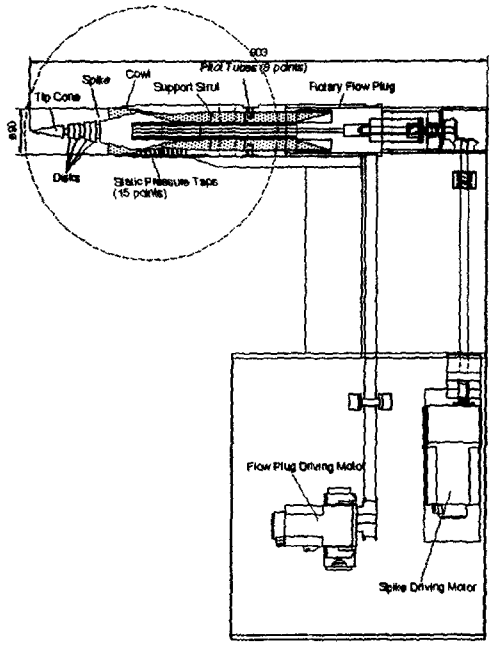

(b) Model tested in ISTA hypersonic wind tunnel.

Fig.9 Schematic drawings of the MRD wind tunnel test models.

tunnel. This model size is 90 mm in cowl inlet diameter. The centerbody of this model can be translated forward and backward by servomotor. The flow plug, which controls back pressure of the inlet model, can be driven by another servomotor. The spike is composed of a tip cone, several disks arranged downstream and a center shank binding these components. In order to make the relation between the incidence position of the oblique shock from the spike tip into the cowl and MCR clear, boundary layer bleed was not conducted in this test.

The MRD inlet centerbody that has several cavities on its surface with keeping design centerbody length is designated as 'stripped centerbody'. The MRD inlet centerbody, whose length is longer than

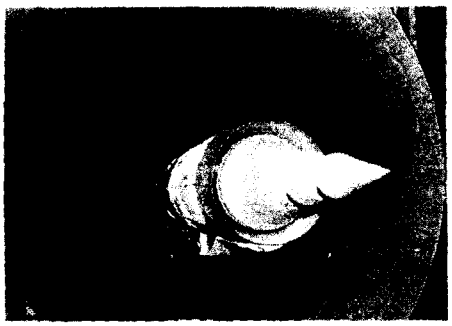

Fig.10 Photograph of the MRD inlet model installed in ISTA wind tunnel.

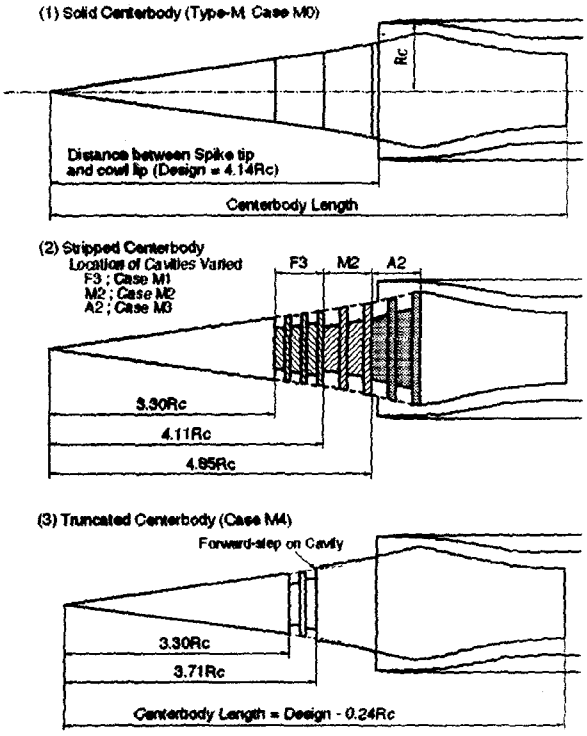

Fig.11 Tested geometries of a stripped centerbody and a truncated centerbody.

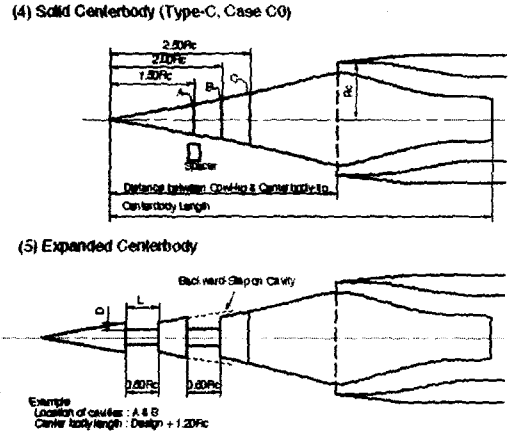

Fig.12 Tested geometries of an expanded centerbody.

design length by making disk spacing wide, is designated as 'expanded centerbody'. On the contrary, the centerbody, whose length is shorter than design length by making disk spacing narrow, is designated as 'truncated centerbody'. It is noted that cavities formed on surfaces of the expanded centerbody and the truncated centerbody have steps as shown in Fig.11 and Fig.12. The inlet geometry designated 'Type-M[15]' is adopted as the base geometry of the inlet with the stripped centerbody and the truncated centerbody and 'Type-C[16]' is adopted as the base geometry of the inlet with the expanded centerbody. Both Type-C and Type-M inlet model were designed in ISAS. Specifications of two inlet geometries, Type-C and Type-M, are shown in Table.2. Both inlet geometries are so designed as to meet shock-on-lip condition at design Mach number. Figure 11 shows tested geometries of the stripped centerbody and the truncated centerbody. Cavity L/D of the stripped centerbody is 1.0 based on findings on characteristics of the conical cavity flow. The expanded centerbody geometries are formed by insertion of spacers into the solid centerbody at locations marked as A, B and C in Fig.12.

TPR and MCR are two important parameters of evaluating inlet performance. In this test, TPR is defined as follows;

$$TPR = P_1 / P_0,$$

where P_1 is an average of exit total pressure measured by using 8 pitot tubes installed at 272.5 mm from the cowl lip, and P_0 is chamber pressure of the wind tunnel. MCR is defined as follows;

$$MCR = \dot{m} / (\rho u A),$$

where $\dot{m}$, ρ, u and A indicate a mass flow rate of the incoming air into the inlet, the density of the free stream, the velocity of free stream, the cowl entry sectional area respectively. We measured the mass flow rate, $\dot{m}$ by using total pressure and static pressure at 272.5 mm from the cowl lip. We determined a flow coefficient with results of CFD. In order to verify the CFD results, cowl static pressure distribution was measured.

Specification of the wind tunnels and test conditions are summarized in Table.3.

Experimental Results

Experimental results are summarized in Table.4. Fig.13 shows a Schlieren image of the flow field around the MRD inlet with the stripped centerbody (test case No. a-2). The inlet performance of the MRD inlet with the stripped centerbody is equal to that of a conventional inlet with solid centerbody when location of cavities is F2 or M2, except for A2 as shown in Table.4. This result also says that the MRD inlet with the stripped centerbody excels the conventional inlet in the viewpoints of structure lightness and simplicity.

Figure 14 shows a Schlieren image of the flow field around the MRD inlet with the truncated centerbody (test case No. b-2). It is observed that a strong bow-shock wave is generated from a cavity with forward-step formed by making disk spacing narrow. Because the throat area cannot be enough small due to this bow-shock wave, TPR of the MRD inlet is deteriorated by 5.5 % compared with the conventional inlet with the solid centerbody. While

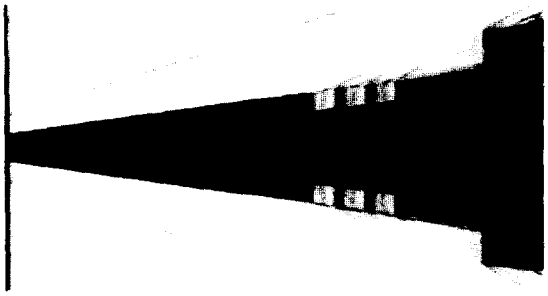

Fig.13 Schlieren image of the MRD inlet with a stripped centerbody (Test Case No. a-2).

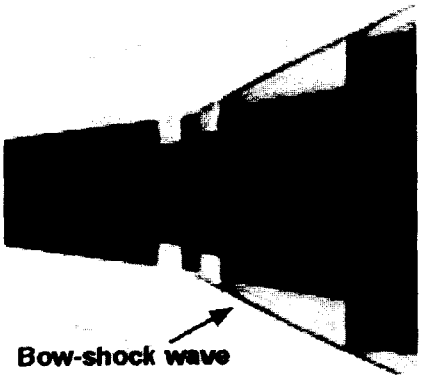

Fig.14 Schlieren image of the MRD inlet with a truncated centerbody (Test Case No. b-2).

(a) Test case No. c-7.

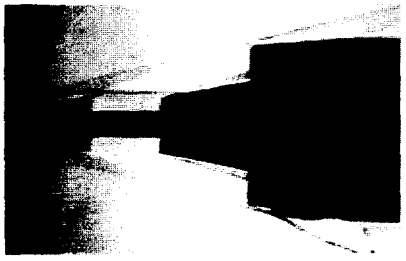

(b) Test case No. c-13.

Fig.15 Schlieren image of the MRD inlet with an expanded centerbody.

the MRD inlet can improve MCR by 2.1 % compared with the conventional inlet owing to reducing the spillage flow with the truncated centerbody. In order to improve the performance of the conventional inlet with the truncated centerbody, reduction of the strong bow-shock wave is necessary.

Fig.15 shows a Schlieren image of the flow field around the MRD inlet with the expanded centerbody ((a) test case No. c-7, (b) c-13). Backward-steps are formed on the cavities of the expanded centerbody surface. Expansion waves generated from leading edge of the cavity and a shock wave from tailing edge are observed.

It is found that the MRD inlet with the expanded centerbody excels a conventional inlet in the ability of matching MCR to a core-engine requiring mass flow rate. Figure 16 compares the performance of the MRD inlet and the conventional inlet at Mach 3.5. Because the conventional inlet cannot control the compression ratio and MCR independently, TPR must be decreased due to the excessive throat area by translating the overall centerbody forward in order to change MCR. While the MRD inlet can change MCR with keeping higher TPR than that of the conventional inlet because of the function of controlling the compression ratio and MCR independently. At Mach 3.5, the MRD inlet can improve TPR by about 10 % compared with the conventional inlet under off-design MCR conditions. Figure 17 compares the performance of the MRD inlet and a conventional inlet at Mach 5.1. The inlet models (both the conventional inlet and the MRD inlet) keep start condition even though the oblique shock from the spike tip enters the cowl. Therefore, the conventional inlet cannot reduce MCR even though the overall centerbody is translated pretty forward. Thus it is said that the conventional inlet with the solid centerbody cannot change MCR at higher Mach number than that makes shock-on-lip condition. On the other hand, the MRD inlet can change MCR with keeping higher TPR at Mach 5.1. It is also noted that TPR of the MRD inlet is kept high in case that the cavity L/D on the expanded centerbody (test case No. c-15) is large (= 6.0) .

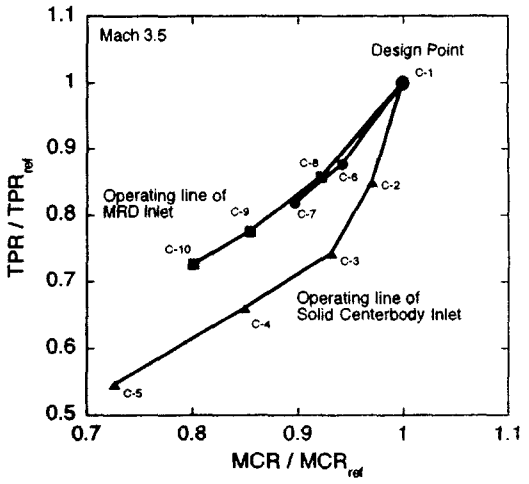

Fig. 16 The off-design MCR performances of the MRD inlet and the conventional inlet at Mach 3.5.

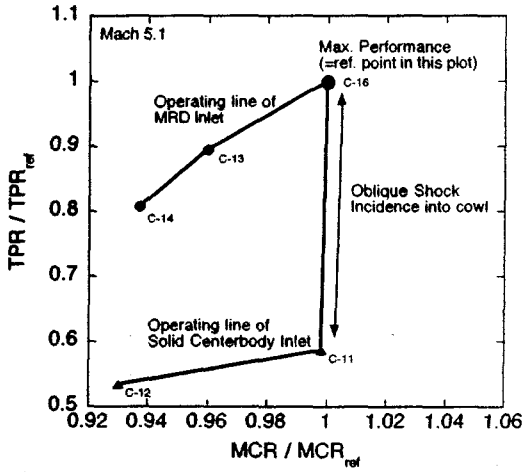

Fig. 17 The off-design MCR performances of the MRD inlet and the conventional inlet at Mach 5.1.

Concluding Remarks

We invented a new supersonic axi-symmetric air inlet, that is the Multi-Row Disk inlet, which can improve the off-design performance of conventional axi-symmetric air inlets because of its ability of controlling the compression ratio and mass capture ratio independently, which conventional axi-symmetric air inlets do not have. Two kinds of wind tunnel tests were conducted to investigate characteristics and verify the function of the MRD inlet. Following findings are acquired.

- Cavities whose L/Ds are less than 1.0 have little negative effect on the growth of the boundary layer.
- Cavity L/D is a dominant factor of the boundary layer growth downstream of the cavities, whereas the number and the size of cavities are not effective compared with the cavity L/D.
- The performance of the MRD inlet with several cavities whose L/Ds are equal to 1.0, that is the MRD inlet with the stripped centerbody, are equal to that of the conventional axi-symmetric air inlet with the solid centerbody. The MRD inlet with the stripped centerbody excels the conventional inlet in the viewpoints of structure lightness and simplicity.
- The MRD inlet with a truncated centerbody improves MCR by 2.1%, however TPR of the MRD inlet deteriorates by 5.5% because of a bow-shock wave generated from forward-steps on the cavities.
- The MRD inlet can improve TPR by about 10 % compared with the conventional inlet under off-design MCR condition at Mach 3.5.

Acknowledgement

The authors gratefully acknowledge the contribution of Mr. Hongoh (ISAS), Mr. Negoro, Mr. Yamaji (graduate student, the university of Tokyo), Ms. Irikado (ISAS), Mr. Tsuda and all members of ISTA hypersonic wind tunnel team for their support.

References

1) Sato, T.: Development Study of the ATREX Engine, IAC-03-S.5.02, 54th International Astronautical Congress, Bremen, Oct 2003.
2) Gary L. Cole: Wind Tunnel Evaluation of YF-12 Inlet Response to Internal Airflow Disturbances with and without Control, NASA CP-2054, 1978.
3) Joseph F. Wasserbauer: Distortion in a Full-Scale Bicone Inlet with Internal Focused Compression and 45 percent Internal Contraction, NASA TM X-3133, 1974.
4) Ge-Cheng Zha: Investigations of High-Speed Civil Transport Inlet Unstart at Angle of Attack, *J. Aircraft*, Vol.35, No.6, 1998.
5) Takagi, I.: Development Study on Air Intake for ATREX Engine, International Symposium on Air Breathing Engines, ISABE 97-7031, International Society for Air Breathing Engines, June 1997.
6) Kojima, T.: Development Study on Axisymmetric Air Inlet for ATREX Engine, AIAA 2001-1895, 10th AIAA/NAL/NASDA/ISAS International Space Planes and Hypersonic Systems and Technologies Conference, Kyoto, 2001.
7) 小島孝之: ATREX エアインテークの研究開発, 第 40 回航空原動機・宇宙推進講演会講演集, 2000, pp. 263-268.
8) Kobayashi, H.: Air Intake and Intake System, Japanese Patent 2003-016096 (Patent Pending), 2003.
9) 丸祐介: 超音速インテークの圧縮面上における境界層制御に関する研究, 第 43 回航空原動機・宇宙推進講演会講演集, 2003, pp. 213-218.
10) Kobayashi, H.: Experimental Study of Multi-Row Disk Inlets for Hypersonic Air Breathing Propulsion, AIAA 2004-861, 42nd AIAA Aerospace Sciences Meeting and Exhibit, Reno Nevada, January 2004
11) Robert L. Stalling: Experimental Cavity Pressure Distortions at Supersonic Speeds, NASA TP-2683, 1987.
12) K. Sakamoto: Experimental Investigation of Supersonic Internal Cavity Flows, AIAA 95-2213, 1995.
13) Richard J. Margason: Effect of Two-Dimensional Cavities on Boundary Layers in Adverse Pressure Gradients, AIAA 97-0300, 1997.
14) 村上哲: 超音速内部流におけるキャビティ抽気及びその形状の空力特性への影響, 航空宇宙技術研究所報告 1247 号, 1994.
15) 勘田将生: 軸対称型エアインテークの設計に関する研究, 第 41 回航空原動機・宇宙推進講演会講演集, 2001.
16) Smeltzer, D. B.: Investigation of a Mixed-Compression Axisymmetric Inlet System at Mach Numbers 0.6 to 3.5, NASA-TN-D-6078, 1970.
17) Sdon, J.: *Intake Aerodynamics*, AIAA Educational Series, Washington D. C., 1989.

Table. 1 Tests conditions summary.

Test Conditions	
Test Section Geometry	0.6 [m] × 0.6 [m]
Free Stream Mach Number	3.0
Test Duration Time [sec.]	90
Chamber Pressure, P_0 [MPa]	0.441
Chamber Temperature, T_0 [K]	288
Free Stream Re Number [m^{-1}]	3.48×10^7
Cavity Parameters	
Cavity L/D	L/D = 0.5, 1.0, 3.7
Cavity Size	D = 5mm, 15mm, 25mm
Number of Cavities	1, 2, 6

Table.2 Specifications of inlet geometry.

	Type-C	Type-M
Design Mach Number	3.5	5.3
Shock-on-Lip Mach Number	3.5	5.3
Spike Tip Half-Cone-Angle	10 deg.	8 deg.
Distance between Spike tip and Cowl lip	2.84Rc @ M3.5, Design Point	4.14Rc @ M5.3, Design Point

Rc : Cowl Radius (45 mm in this model)

Table.3 Specifications of wind tunnels and test conditions.

	ISAS Supersonic Wind Tunnel		ISTA Hypersonic Wind Tunnel
Test Section Geometry	0.6 [m] × 0.6 [m]		ϕ 0.5 [m]
Free Stream Mach Number	3.5	4.0	5.1
Test Duration Time [sec.]	50	40	60
Chamber Pressure, P_0 [MPa]	0.663	0.510	1.0
Chamber Temperature, T_0 [K]	288	288	650
Free Stream Re Number [m^{-1}]	4.06×10^7	2.45×10^7	8.43×10^6

Table.4 Results of validation tests of the MRD inlet summary.

Test Case No.	Mach No.	Geometry Case No.	Centerbody Length	Location of cavities	Cavity L/D	Distance between Spike tip and Cowl lip	TPR/TPRref	MCR/MCRref	
(a) Stripped Centerbody (Base inlet geometry: Type-M)									
a-1	3.5	M0	Design	Nothing (Solid)	-	Design + 0.56 Rc	1.000	1.000	ref. in (a)
a-2	3.5	M1	Design	F3	1.0	Design + 0.55 Rc	1.002	0.996	
a-3	3.5	M2	Design	M2	1.0	Design + 0.55 Rc	1.006	1.000	
a-4	3.5	M3	Design	A2	1.0	Design + 0.98 Rc	not acquired	0.504	
(b) Truncated Centerbody (Base inlet geometry: Type-M)									
b-1	4.0	M0	Design	Nothing (Solid)	-	Design + 0.50 Rc	1.000	1.000	ref. in (b)
b-2	4.0	M4	Design - 0.24 Rc	Shown in Fig.11	-	Design + 0.34 Rc	0.945	1.021	
(c) Expanded Centerbody (Base inlet geometry: Type-C)									
c-1	3.5	C0	Design	Nothing (Solid)	-	Design + 0.25 Rc	1.000	1.000	ref. in (c)
c-2	3.5	C0	Design	Nothing (Solid)	-	Design + 0.37 Rc	0.850	0.970	
c-3	3.5	C0	Design	Nothing (Solid)	-	Design + 0.51 Rc	0.743	0.931	
c-4	3.5	C0	Design	Nothing (Solid)	-	Design + 0.71 Rc	0.660	0.849	
c-5	3.5	C0	Design	Nothing (Solid)	-	Design + 0.90 Rc	0.545	0.724	
c-6	3.5	C1	Design + 0.20 Rc	B	1.0	Design + 0.48 Rc	0.878	0.942	
c-7	3.5	C2	Design + 0.40 Rc	B	2.0	Design + 0.68 Rc	0.817	0.897	
c-8	3.5	C3	Design + 0.20 Rc	C	0.8	Design + 0.51 Rc	0.858	0.922	
c-9	3.5	C4	Design + 0.40 Rc	C	1.4	Design + 0.71 Rc	0.776	0.854	
c-10	3.5	C5	Design + 0.60 Rc	C	2.2	Design + 0.91 Rc	0.726	0.801	
c-11	5.1	C0	Design	Nothing (Solid)	-	Design + 0.87 Rc	0.185	0.998	
c-12	5.1	C0	Design	Nothing (Solid)	-	Design + 0.98 Rc	0.168	0.930	
c-13	5.1	C6	Design + 0.80 Rc	B	4.0	Design + 1.06 Rc	0.282	0.960	
c-14	5.1	C7	Design + 1.20 Rc	A & B	A: 4.6, B: 3.0	Design + 1.51 Rc	0.254	0.937	
c-15	5.1	C8	Design + 1.20 Rc	A & B	A: 4.6, B: 6.0	Design + 1.51 Rc	0.257	0.937	
c-16	5.1	C0	Design	Nothing (Solid)	-	Design + 0.07 Rc	0.315	1.000	